2019

The Sucking Louse Fauna of Mongolian Rodents: Host Associations, Molecular Phylogenetics and Description of Two New Species

Chase N. Robinson
Georgia Southern University

The Sucking Louse Fauna of Mongolian Rodents: Host Associations, Molecular Phylogenetics and Description of Two New Species

An Honors Thesis submitted in partial fulfillment of the requirements for Honors in Biology.

By
Chase Robinson

Under the mentorship of Dr. Stephen Greiman and Dr. Lance Durden

ABSTRACT

This study aimed to screen Mongolian rodents for sucking lice (Insecta: Phthiraptera: Anoplura) to better understand host-parasite associations for this understudied region. Nine species, including 3 previously undescribed, from 4 genera were identified. A molecular phylogeny based on 2 mitochondrial genes of collected louse specimens is included.

Thesis Mentor:_____

Dr. Stephen Greiman

Thesis Mentor:_____

Dr. Lance Durden

Honors Director:_____

Dr. Steven Engel

April 2019
Department of Biology
University Honors Program
Georgia Southern University

Acknowledgements

I would like to thank Georgia Southern University's Honors Program for the opportunity to complete this capstone project. I would also like to thank the Department of Biology for the use of the Scanning Electron Microscope and facilities. I thank my faculty advisors Dr. Stephen Greiman and Dr. Lance Durden for their constant support and guidance throughout this experience. Finally, I would like to thank my fellow laboratory colleagues Sara Cowan, Briana Sesmundo, and Ashley Passantino.

Introduction

More than 530 species of sucking lice (Insecta: Phthiraptera: Anoplura) have been described from at least 830 different species of mammals globally (Durden and Musser, 1994). Knowledge of the sucking louse fauna from Mongolia has previously only been recorded through individual expeditions and collections. Studies of the lice of Mongolia include KÉLER (1966) who identified eight species of sucking lice belonging to four genera, *Hoplopleura, Polyplax, Neohaematopinus* and *Eulinognathus*, during the Mongolian-German Biological Expedition of 1964. Differentiation of new species was reported not to be possible because most lice were only identified to genus. KRIŠTOFŠÍK (1999) reported sucking lice from 20 mammal species in Mongolia and noted 1,199 sucking lice belonging to 21 different species and 6 genera, *Enderleinellus, Hoplopleura, Eulinognathus, Linognathoides, Neohaematopinus*, and *Polyplax*. Geographical distributions included lice from 4 regions in Mongolia with 14 species being recorded from Mongolia for the first time. The lice reported in both studies parasitize various species of rodents throughout Mongolia. Due to climate and terrain, many regions of Mongolia have not seen adequate scientific sampling and remain untapped.

Mongolia is a region in which information on rodent lice is close to non-existent. Predating this paper, species descriptions are limited, commonly lack visual descriptions, and have no molecular data. Therefore, this study will allow for the expansion of a molecular baseline via gene sequencing and a molecular phylogeny. No previous molecular studies have been conducted regarding sucking lice from Mongolia. Also, the enhancement of the baseline knowledge of the species collected in this study will allow

for more precise future species descriptions. In continuation, morphological information regarding specimens was collected with the use of scanning electron microscopy. It is important to document new taxa to increase the knowledge of ectoparasite biodiversity and to more thoroughly understand the relationship between hosts and parasites. It is also critical to incorporate molecular data to better understand their evolutionary history. In this study, we describe two new species of lice from the genera *Hoplopleura* and *Linognathoides*, as well as, characterize the evolutionary relationship amongst collected lice taxa utilizing a molecular phylogeny.

Methods

Sample Collection

Small Mongolian mammals were collected from 10 areas in Arkhangai, Bayan-Olgii, Khovsgol, and Uvs provinces in Mongolia from July to August 2015. These specimens were a part of a larger study examining the diversity and coevolution of northern latitude mammals and their parasites (Cook et al., 2017). Specimens were collected following field methods (Galbreath et al., 2019) and guidelines of the institutional animal care and use committees (IACUC) as well as the American Society of Mammologists Guide for Use of Wild Mammals in Research (Sikes et al., 2011). Lice were collected using forceps and immediately stored in 95% ethanol following removal from host. The host mammals were gathered using guidelines set by the institutional animal care and use committees, as well as the American Society of Mammologists Guide for Use of Wild Mammals in Research (Sikes et al., 2011), and are stored at the Museum of Southwestern Biology.

DNA Extraction

Individual louse specimens were removed from 80% ethanol storage and punctured with an Austerlitz 000 Insect Pin in the anterior ventral end of the abdomen. Each sample was placed in a 1.5 ml microcentrifuge tube containing a solution of 95 µl digestion buffer, 95 µl water, and 10 µl proteinase K (Zymo Research, Irvine, CA) and left in Fisher Biotemp® Incubator overnight. The louse exoskeletons were then removed from the lysate solution and placed into 80% ethanol, while adding 200 µl of isopropyl alcohol to precipitate out the DNA, to the remaining lysate solution. Both the louse exoskeletons and DNA lysate solutions were placed in a -20°C freezer. Lice exoskeletons were directly slide mounted as permanent morphological vouchers.

DNA extraction was completed following Tkach and Pawloski (1999). In short, after precipitation in the freezer, the DNA lysate solutions were centrifuged at 15,000 rpm for 15 min. Supernatant was removed and 180 µl of 70% ethanol was added and vortexed. Solutions were centrifuged at 15,000 rpm for 5 minutes followed by the removal of supernatant. Next 180 µl of 70% ethanol was added, vortexed, and centrifuged at 15,000 rpm for 5 minutes. Supernatant was removed, and specimens were placed on heat block for 20 minutes at 60 °C. After the remaining ethanol had evaporated 40 µl of water was added to suspend the DNA and stored at -20°C for later work.

Amplification and Sequencing

DNA fragments approximately 600-base-pair-long of the 18S rRNA gene, approximately 450-base-pair-long fragments of the 12S rrnS gene, and approximately 400-base-pair-long fragments of the 16S rrnL gene were amplified on a SimpliAmp Thermocycler using GoTaq Colorless Master Mix from Promega Corporation (Madison,

Wisconsin) for 54 lice samples. The two primers used for 18S amplification were the forward primer NS1 and the reverse primer NS2a (Barker et al., 2003); 12S amplification were the forward primer 12SA and reverse primer 12SB (Dong et al., 2014); 16S amplification were the forward primer 16SF and reverse primer Lx16SR (Dong et al., 204).

Primers used for 12S and 16S amplifications were ordered via Eurofins Genomics (Louisville, Kentucky) and re-suspended upon arrival. Primer concentrations of 10 ρM and 2 ρM were used for PCR and sequencing respectively.

The 18S profile of the thermocycler was as follows: initial denaturation at 95°C for 2 minutes, followed by 40 cycles of 95°C for 35 seconds, 50°C for 45 seconds, and final extension at 72°C for 5 minutes respectively. The 16S profile of the thermocycler was as follows: 95°C for 2 minutes, followed by 40 cycles of 95°C for 35 seconds, 50°C for 45 seconds, and final extension at 72°C for 5 minutes respectively. The 12S profile of the thermocycler was as follows: 95°C for 2 minutes, followed by 40 cycles of 95°C for 35 seconds, 50°C for 45 seconds, and final extension at 72°C for 5 minutes respectively After completion, PCR products were held at 10°C until removal from thermocycler.

The PCR products were purified using ExoSap PCR clean-up enzymatic kit from Affimetrix (Santa Clara, California). For 18S amplification, Zymoclean™ Gel DNA Recovery Kit from Zymo Research (Irvine, California) was used for additional purification of desired DNA fragments. PCR products were sequenced using ABI Big Dye™ Chemistry (Applied Biosystems, Foster City, California) on an ABI 3500 capillary sequencer using the original primers from PCR amplification. The sequences obtained were compiled and edited using Geneious 11.01 (Newark, New Jersey). Initial primer

binding sequences were removed, and any areas of uncertainty were verified or corrected to increase sequence validity. Complete sequences were submitted to the National Center for Biotechnology Information (NCBI).

Phylogenetics

Compiled and edited DNA sequences on Geneious 11.01, along with available DNA sequences of lice from families of Anoplura submitted to NCBI's GenBank, were aligned using the multiple align tool. Aligned sequences were saved as a FASTA file and submitted to the Castesana Lab Gblocks Server (Institut de Biologia Evolutiva, Barcelona, Spain) for elimination of poorly aligned and ambiguous regions for more accurate phylogenetic analysis. The reduced DNA alignment was used for a phylogenetic analysis using MrBayes V3.1 on the Cyberinfrastructure for Phylogenetic Research (CIPRES).

Slide Mounting

Extracted louse specimens were slide mounted using Polyvinyl Alcohol (PVA) mounting medium (Bioquip Products, Rancho Dominguez, California). One drop of PVA Mounting Medium was placed on a microscope slide, and each specimen was coverslipped with a 10 mm circular cover slip. Individual lice were removed from 95% ethanol and placed into the mounting medium on the microscope slide. Specimens were then ventrally orientated using a small metal probe. For louse specimens that were not utilized for DNA extraction, individuals were cleared for approximately 24 hours in potassium hydroxide, following puncture of the ventral abdomen with a 000 insect pin. Lice were then dehydrated through an ethanol series with a final dehydration step in xylene. The mounting process remained the same, only utilizing Canada balsam instead

of PVA. Slide mounted specimens were placed directly into an oven at 50°C after initial mounting for curing. Permanent slide labels were created using Microsoft® Office Word, addressing key components for host and louse collection.

Scanning Electron Microscopy

Male and female lice of the *Hoplopleura* n. sp. were imaged on a Scanning Electron Microscope (SEM) as follows. The specimens were dehydrated in a graded ethanol series, starting with 70% for 30 minutes, followed by 80% for 30 minutes, 90% for 1 hour, 95% overnight, and 100% for 24 hours respectively. After dehydration, chemical dehydration was completed by a graded series of ethanol/hexamethyldisilazane (HMDS). The series began with 2:1 (Ethanol: Hexamethyldisilazane) for 2 hours, followed by 1:1 for 2 hours, 1:2 for 3 hours, 1:3 overnight, and pure HMDS respectively. The chemically dried specimens were mounted on an aluminum stub, sputter coated with gold/palladium in the presence of Argon gas and viewed on a JOEL JSM-6610. Multiple high magnification images were taken of each whole specimen and later stitched together using photomerge on Adobe Photoshop CC.

Light Microscopy Digital Imaging

Permanent slide mounts of the new species and representatives of identified lice genera were digitally imaged using a Nikon Eclipse Ni-U research microscope equipped with a Nikon DS-L3 camera (Nikon Inc., Melville, New York). Slides were positioned appropriately, along with light and balance enhancement to provide the most accurate rendering of the lice. Similar to the Scanning Electron Microscopy imaging, individual images were stitched together using photomerge and edited on Adobe Photoshop CC.

Line Drawings

Slide mounted specimens were examined using the 100x-400x objectives on an Olympus BH-2 phase contrast high-power microscope (Olympus Corporation of the Americas, Center Valley, Pennsylvania) connected to an Ikegami MTV-3 video camera attachment and monitor (Ikegami Electronics, Neuss, Germany). Specific measurements were made using a calibrated ocular micrometer. Drawings also utilized imaging from scanning electron microscopy and light microscopy digital imaging. Initial images were created using pencil but finalized using ink pen and a light table.

Adobe Photoshop CC

This program was used to allow for the more efficient and detailed images of the louse species to be achieved. Images for both the Scanning Electron Microscope and the light microscopy digital imaging were taken at a higher magnification in a grid like pattern. The individual images were stitched together with editing using the photomerge program. Unnecessary objects, such as dirt and host tissues, were removed with the bandage tool with no effect to the structure or composition of bodily objects. Also, the background of the images were homogenized using the stamp tool to allow for a greater focus of the louse morphology. Scale bars were drawn in using shape tools, based on measurements from the light microscopy digital imaging. Images were then combined together, including line drawings, to form image plates for accurate presentation.

Species Descriptions

Names of anopluran morphological structures, including setae, follow Kim and Ludwig (1978) and Durden et al. (2018).

Results

Initially, the screening of Mongolian rodents for sucking lice was conducted from a total of 198 collected specimens. Of the 198 lice, 56 were selected for DNA extraction and species identification. The identified species were collected from 10 genera of rodents located in 10 geographical locations in Mongolia. Species of rodents include *Alticola barakshin, Alticola strelzowi, Urocitellus undulatus, Ellobius tancrei, Myodes rutilus, Meriones meridinaus, Cricetulus longicaudatus, Allocricetulus curatus, Myodes rufocanus, Microtus oeconomus, Microtus gregalis, Cricetulus barabensis,* and *Tamias sibricus*. Localities of host collections include the following Mongolian provinces: Uvs, Bayan-Olgii, Khovsgol, Arkhangai. Identified lice include the following: *Hoplopleura* n. sp., *Linognathoides* n. sp., *Polyplax* n. sp., *Polyplax ellobii, Hoplopleura acanthopus, Polyplax meridiaus, Polyplax dentaticornis, Polyplax qiuae,* and *Enderleinellus tamiasis*. Host-parasite relationships and specific localities of collections with geographic coordinates are provided in Table 1.

Based on adequate sample sizes two new species of Anoplura were selected for descriptions: *Linognathoides urocitelli* n. sp. (Anoplura Polyplacidae) from the long-tailed ground squirrel *Urocitellus undulates* and *Hoplopleura* n. sp. (family Hoplopleuridae) from the Gobi Altai mountain vole *Alticola barakshin* and the Flat-headed vole *Alticola strelzowi*. The thirds new species *Polyplax* n. sp. (family Polyplacidae) from the northern red-backed vole *Myodes rutilus* was represented by only female specimens and will be described separately when male specimens have been collected.

A molecular phylogeny of identified louse specimens is included. Phylogenetic relationships of 13 Mongolian sucking lice resulting from Bayesian analysis of concatenated gene fragments from 16S rrnL and 12S rrnS can be seen in Figure 5. The limited resulting phylogenetic tree, formed through Bayesian analysis, showed high support for the central clade including all identified specimens of *Hoplopleura acanthopus*. The clade of *Hoplopleura acanthopus* correlated geographic distribution with relatedness. Individuals collected from relatively close localities show higher levels of relatedness when compared to those collected from other localities. In terms of new species, the *Hoplopleura* n. sp. specimens form a sister clade to that of *Hoplopleura acanthopus*. Both *Hoplopleura* n. sp. individuals shared the same host and collection localities. The *Linognathoides urocitelli* n. sp. forms a sister clade to the *Hoplopleura* clade, which showed 100% support. *Polyplax elobii* was determined to be within the same clade as *Pediculus humanus capitis*. The outgroup was reinforced to be *Haematozymus elephantis*.

Description of *Linognathoides urocitelli*, n. sp.

(Figs. 1-3)

Male (Figs. 1A-D, 2A,B) (n=1): Total body length of Holotype, 1.128 mm. Head, thorax and abdomen moderately sclerotized.

Head (Figs. 1A, 2A): Slightly longer than wide with broadly curved lateral margins posterior to antennae and extended medio-anteriorly; maximum head width, 0.190 mm. Antennae 5-segmented with broad basal segment and elongated second segment; third segment not highly modified. One distinct VPHS, 2 Sutural Head Setae

(SHS), 4 Dorsal Marginal Head Setae (DMHS), 1 Dorsal Anterior Central Head Seta (DAnCHS), 1 Dorsal Posterior Head Seta
(DPoHS), 1 extremely long Dorsal Principal Head Seta (DPHS), 1 small Dorsal Accessory Head Seta (DAcHS), 2 Supraantennal Head Setae (SpAtHS), 1 small Dorsal Preantennal Head Seta, and 4 Apical Head Setae (ApHS) on each side.

Thorax (Figs. 1A, 2A): Broader than head; maximum thorax width, 0.260 mm. Thoracic sternal plate (Fig. 1B) subeliptical, broadly rounded anteriorly and laterally, and with distinct posterior extension. Thoracic fragma distinct. Mesothoracic spiracle diameter, 0.018 mm. Dorsal Principal Thoracic Seta (DPTS) length, 0.105 mm. Legs each terminating in tibio-tarsal acuminate claw; forelegs distinctly smaller than other legs; midlegs slightly smaller than hindlegs; leg coxae subtriangular with small postero-lateral extensions on second and third
coxae.

Abdomen (Figs. 1A, 2A): Broader than thorax with 8 narrow, short tergites and 5 narrow, short sternites. Eight rows of 5-8 long Dorsal Central Abdominal Setae (DCAS) – each row associated with abdominal segment; rows 2-8 each associated with tergites. Seven rows of 1-3 long Dorsal Marginal Abdominal Setae (DMAS) on each side; row 1 with 1 DMAS on each side, rows 2-6 each with 3 DMAS on each side, and row 7 with 2 DMAS on each side. Fourteen rows of Ventral Central Abdominal Setae (VCAS), each with 2-6 VCAS; 2 rows of long VCAS associated with each abdominal segment anterior to subgenital plate; 6 rows of 2-6 long Ventral
Marginal Abdominal Setae (VMAS); rows 1 and 4 each with 2 VMAS on each side, rows 2 and

3 each with 3 VMAS on each side, rows 5 and 6 each with 1 VMAS on each side.

Paratergal plates (Figs. 1C, 2A): Present on abdominal segments II-VIII; plates on segments II-VII subtriangular; plates on segments III-VII each with spiracle; plates differentially sclerotized. Plate on abdominal segment II with 1 long seta and 1 seta of moderate length; plates on segments III and IV each with 1 very long seta and 1 seta of moderate length; plates on segments V and VI each with 2 setae of moderate but slightly different lengths; plates on segments VII and VIII each with 2 very long setae.

Genitalia (Figs. 1D, 2B): Basal apodeme slightly longer than parameres. Postero-lateral angles of basal apodeme acute with curved convex posterior margin between angles; parameres broadly curved, each with small antero-medial hook-like process; lateral margins of pseudopenis distinctly dentate; apex of pseudopenis extending slightly beyond posterior confluence of parameres. Subgenital plate (Fig. 1A) extending anteriorly to abdominal segment VI, with almost straight anterior margin, curved lateral margins, and tapering posteriorly; 2 distinct lacunae present, anterior lacuna elongated bilaterally, posterior lacuna larger with almost straight anterior margin and curved, tapering, posterior-lateral margin.

Female (Figs. 2C, 3A-D). (n=3). Total body length of allotype, 1.600 mm; mean, 1.507 mm; range, 1.445-1.600 mm.

Head, thorax and abdomen as in male unless indicated otherwise.

Head (Figs. 2C, 3A): Maximum head width of allotype, 0.211 mm; mean, 0.210 mm; range, 0.205-0.215 mm.

Thorax (Figs. 2C, 3A): Thoracic sternal plate (Fig. 3B) with slightly shorter, less acute posterior extension than in male. Maximum thorax width of allotype, 0.295 mm;

mean, 0.308 mm; range, 0.295-0.325 mm. DPTS length of allotype, 0.145 mm; mean, 0.141 mm; range, 0.138-0.145 mm. Mesothoracic spiracle diameter of allotype, 0.022 mm; mean, 0.020 mm; range, 0.018-0.022 mm.

Abdomen (Figs. 2C, 3A): Lacking tergites and sternites except for ventral subgenital plate. Fourteen rows of 6-10 long DCAS; 12 rows of 3-4 DMAS on each side, rows 1-4 and 12 each with 3 setae on each side and rows 5-11 each with 4 setae on each side. Twelve rows of 416 long VCAS; 10 rows of 3 VMAS on each side. Some abdominal setae dagger-shaped, especially on ventral surface.

Paratergal plates (Figs. 2C, 3C): Differential sclerotization and lengths of apical setae on plates of abdominal segments IV and V slightly different than in male as shown in Fig. 3C. Number of shorter apical setae on paratergal plates on segments II and III slightly variable: on plate of segment II, allotype female has 1 shorter seta on 1 side and 2 on the other side; 2 paratype females have 2 shorter setae on both sides; on plate of segment III, allotype female and 1 paratype female have 1 shorter seta on both sides; another female paratype has 1 shorter seta on 1 side and 2 on the other side.

Genitalia (Fig. 3D): Subgenital plate subrectangular, much wider than long, with slightly concave, irregular anterior margin and slightly concave, smoothly rounded posterior margin; with single large central lacuna and 2 small central setae anterior to lacuna. Three-4 small setae anterior to gonopod VIII on each side. Gonopods VIII irregularly shaped and medially situated, each with 1 longer medial seta and 1 shorter lateral seta. Gonopods IX less distinct and more lateral than gonopods VIII, each with 2 rows of 3 long setae, followed by 1 short stout seta. ~Six small setae on each side adjacent to gonopods.

NYMPH (third instar) (Fig. 2D). (n=1). Total body length of Paratype nymph, 1.170 mm. Overall body shape wider than in adults.

Head: Broadly rounded anteriorly with small antero-medial projection; lateral margins almost straight posterior to antennae. Maximum head width, 0.201 mm. Ventrally, 1 anterolateral denticle, 1 antero-medial denticle, and pair of denticles just medial to 1st antennal segment on each side; 1 denticle near mediolateral margin of first antennal segment on each side. Four
DMHS, 2 SuHS, 1 long DPTS and 1 short DAcHS both borne on small protuberance, 1 SpAtHS, 1 DPaHS, 4 ApHS, 1 VPHS and 1VPaHS on each side. Antennae 5-segmented; first segment much longer than wide; second segment slightly wider than long; thirs and fourth segments about as long as wide; fifteh segment tapering distally.

Thorax: Wider than head; maximum thorax width, 0.262 mm. Overall shape of thorax and legs similar to those in adults except tibio-tarsal leg segments broader. No thoracic sternal plate. DPTS length, 0.122 mm. Mesothoracic spiracle diameter, 0.017 mm.

Abdomen: Wider than thorax; integumental sculpting distinct; some morphological features of developing adult female visible beneath nymphal exoskeleton. Eleven rows of 2-5 long DCAS. Eight rows of DLAS; rows 1, 3 and 5 each with 2 long setae, row 2 with 2 long and 1 shorter seta, rows 4 and 6 each with 1 long seta, and rows 7 and 8 each with 1 small seta, on each side.
Seven rows of 2-5 long VCAS. Five rows of long VLAS each with 1-2 VLAS on each side.

Paratergal plates: Eight lightly sclerotized plates present on each side associated with abdominal segments II to IX. Plates on segments II and IX small and irregularly shaped; plates on segments III-VI each subtriangular and produced postero-laterally on 1 side; plates on segments VII and VIII both subrectangular. Plate on abdominal segment II with 1 long apical seta; plates on segments III and IV each with 1 very long seta and 1 shorter seta; plates on segments V and VI each with 1 short seta; plates on segments VII ad VIII each with 2 long setae; plate IX with 1 long and 1 short seta. Spiracles present on each of plates on abdominal segments

III-VII.

Host Species	Accession Number	Lice Species	Province	Locality	Collection Date
Allocricetulus curatus	NK 270087	*Hoplopleura acanthopus*	Uvs	6 km NE of Olgii Sum (49.07199604°N, 92.10190102°E)	25-Jul-15
Alticola barakshin	NK 270167	*Hoplopleura* n. sp.	Bayan-Olgii	Zoolon (49.90486°N, 90.11536°E)	28-Jul-15
	NK 270167	*Hoplopleura* n. sp.	Bayan-Olgii	Zoolon (49.90486°N, 90.11536°E)	28-Jul-15
	NK 270167	*Hoplopleura* n. sp.	Bayan-Olgii	Zoolon (49.90486°N, 90.11536°E)	28-Jul-15
	NK 270167	*Hoplopleura* n. sp.	Bayan-Olgii	Zoolon (49.90486°N, 90.11536°E)	28-Jul-15
Alticola strelzowi	NK 270545	*Hoplopleura* n. sp.	Bayan-Olgii	Huljaa River Valley (49.40665299°N, 89.08553101°E)	5-Aug-15
	NK 270545	*Hoplopleura* n. sp.	Bayan-Olgii	Huljaa River Valley (49.40665299°N, 89.08553101°E)	5-Aug-15
Alticola sp.	NK 270107	*Hoplopleura* n. sp.	Bayan-Olgii	Zoolon (48.904556°N, 90.111152°E)	27-Jul-15
	NK 270107	*Hoplopleura* n. sp.	Bayan-Olgii	Zoolon (48.904556°N, 90.111152°E)	27-Jul-15
	NK 270111	*Hoplopleura* n. sp.	Bayan-Olgii	Zoolon (48.90951703°N, 90.11401702°)	27-Jul-15
	NK 270111	*Hoplopleura* n. sp.	Bayan-Olgii	Zoolon (48.90951703°N, 90.11401702°)	27-Jul-15
	NK 270120	*Hoplopleura* n. sp.	Bayan-Olgii	Zoolon (48.90818398°N. 90.11411299°E)	27-Jul-15
Cricetulus barabensis	NK 270661	*Hoplopleura acanthopus*	Uvs	Harhiraa Mountain, Tsunheg (50.03160601°N, 91.641238°E)	8-Aug-15
	NK 272202	*Polyplax queii*	Khovsgol	Heegtsar River Valley (50.53500501°N, 100.529344°E)	19-Aug-15
Cricetulus longicaudatus	NK 270076	*Polyplax elobii*	Uvs	6 km NE of Olgii Sum (49.07223903°N, 92.10056202°E)	25-Jul-15
	NK 270076	*Polyplax dentaticorais*	Uvs	6 km NE of Olgii Sum (49.07223903°N, 92.10056202°E)	25-Jul-15
Ellobius tancrei	NK 270134	*Polyplax elobii*	Bayan-Olgii	Zoolon (48.90418396°N, 90.11613697°E)	27-Jul-15
Meriones meridinaus	NK 270079	*Polyplax meridinaus*	Uvs	6 km NE of Olgii Sum (49.07344602°N, 92.10364002°E)	25-Jul-15
	NK 270079	*Polyplax meridinaus*	Uvs	6 km NE of Olgii Sum (49.07344602°N, 92.10364002°E)	25-Jul-15
Microtus gregalis	NK 270660	*Hoplopleura acanthopus*	Uvs	Harhiraa Mountain, Tsunheg (50.03398002°N, 91.63828799°E)	8-Aug-15
	NK 270442	*Hoplopleura acanthopus*	Bayan-Olgii	Songinot Gol (48.15614001°N, 89.01266797°E)	1-Aug-15
	NK 270442	*Hoplopleura acanthopus*	Bayan-Olgii	Songinot Gol (48.15614001°N, 89.01266797°E)	1-Aug-15
	NK 270687	*Hoplopleura acanthopus*	Uvs	Juveriin Am, Juveriin Gol (49.87038497°N, 91.20137701°E)	9-Aug-15
Microtus oeconomus	NK 270348	*Hoplopleura acanthopus*	Bayan-Olgii	Songinot Gol (48.15734298°N, 89.009438°E)	31-Jul-15
	NK 270348	*Hoplopleura acanthopus*	Bayan-Olgii	Songinot Gol (48.15734298°N, 89.009438°E)	31-Jul-15
	NK 270946	*Hoplopleura acanthopus*	Uvs	Han Huhnii Mountain, Baruun Turuun River Valley (49.455263°N, 94.64772901°E)	14-Aug-15
	NK 270946	*Hoplopleura acanthopus*	Uvs	Han Huhnii Mountain, Baruun Turuun River Valley (49.455263°N, 94.64772901°E)	14-Aug-15
	NK 272167	*Hoplopleura acanthopus*	Khovsgol	Heegtsar River Valley (50.53397002°N, 100.533631°E)	19-Aug-15
	NK 272167	*Hoplopleura acanthopus*	Khovsgol	Heegtsar River Valley (50.53397002°N, 100.533631°E)	19-Aug-15
	NK 272171	*Hoplopleura acanthopus*	Khovsgol	Heegtsar River Valley (50.53462104°N, 100.533771°E)	19-Aug-15
	NK 272171	*Hoplopleura acanthopus*	Khovsgol	Heegtsar River Valley (50.53462104°N, 100.533771°E)	19-Aug-15
Microtus sp.	NK 270431	*Hoplopleura acanthopus*	Bayan-Olgii	Songinot Gol (48.15657503°N, 89.00843804°E)	1-Aug-15
	NK 270440	*Hoplopleura acanthopus*	Bayan-Olgii	Songinot Gol (48.15967198°N, 89.01367103°E)	1-Aug-15
	NK 270440	*Hoplopleura acanthopus*	Bayan-Olgii	Songinot Gol (48.15967198°N, 89.01367103°E)	1-Aug-15
Myodes rutilus	NK 270026	*Hoplopleura acanthopus*	Arkhangai	Nariinii Gol, north side of Tenkiin Tsagaan Lake (48.22522902°N, 99.75049596°E)	22-Jul-15
	NK 270026	*Hoplopleura acanthopus*	Arkhangai	Nariinii Gol, north side of Tenkiin Tsagaan Lake (48.22522902°N, 99.75049596°E)	22-Jul-15
	NK 270012	*Hoplopleura acanthopus*	Arkhangai	Zurkh Mountain (48.13038996°N, 100.093301°E)	21-Jul-15
	NK 270026	*Hoplopleura acanthopus*	Arkhangai	Nariinii Gol, north side of Tenkiin Tsagaan Lake	22-Jul-15
	NK 270356	*Hoplopleura acanthopus*	Bayan-Olgii	Songinot Gol (48.15591998°N, 89.01563197°E)	31-Jul-15
	NK 270356	*Hoplopleura acanthopus*	Bayan-Olgii	Songinot Gol (48.15591998°N, 89.01563197°E)	31-Jul-15
	NK 270667	*Hoplopleura acanthopus*	Uvs	Harhiraa Mountain, Tsunheg (50.02803097°N, 91.63777602°E)	8-Aug-15
	NK 270667	*Hoplopleura acanthopus*	Uvs	Harhiraa Mountain, Tsunheg (50.02803097°N, 91.63777602°E)	8-Aug-15
	NK 270703	*Hoplopleura acanthopus*	Uvs	Juveriin Am, Juveriin Gol (49.86964401°N, 91.20122597°E)	9-Aug-15
	NK 270703	*Hoplopleura acanthopus*	Uvs	Juveriin Am, Juveriin Gol (49.86964401°N, 91.20122597°E)	9-Aug-15
	NK 270866	*Hoplopleura acanthopus*	Uvs	Han Huhnii Mountain, Baruun Turuun River Valley (49.44304001°N, 94.62757196°E)	13-Aug-15
	NK 270866	*Hoplopleura acanthopus*	Uvs	Han Huhnii Mountain, Baruun Turuun River Valley (49.44304001°N, 94.62757196°E)	13-Aug-15
	NK 272186	*Hoplopleura acanthopus*	Khovsgol	Heegtsar River Valley (50.53317801°N, 100.533784°E)	19-Aug-15
Myodes rufocanus	NK 270283	*Hoplopleura acanthopus*	Bayan-Olgii	Songinot Gol (48.15995101°N, 89.01765°E)	30-Jul-15
	NK 270283	*Hoplopleura acanthopus*	Bayan-Olgii	Songinot Gol (48.15995101°N, 89.01765°E)	30-Jul-15
	NK 270974	*Hoplopleura acanthopus*	Uvs	Han Huhnii Mountain, Baruun Turuun River Valley (49.44563697°N, 94.64463199°E)	14-Aug-15
	NK 270974	*Hoplopleura acanthopus*	Uvs	Han Huhnii Mountain, Baruun Turuun River Valley (49.44563697°N, 94.64463199°E)	14-Aug-15
	NK 272149	*Hoplopleura acanthopus*	Khovsgol	Heegtsar River Valley (50.53126602°N, 100.541434°E)	19-Aug-15
Tamias sibricus	NK 272323	*Endoleinellus tamiasis*	Khovsgol	Heegtsar River Valley (50.52980798°N, 100.532903°E)	20-Aug-15
Urocitellus undulatus	NK 270021	*Linognathoides urocitelli* n. sp.	Arkhangai	Zurkh Mountain (48.13958399°N, 100.097669°E)	21-Jul-15
	NK 270581	*Linognathoides urocitelli* n. sp.	Bayan-Olgii	Huljaa River Valley (49.41051202°N, 89.09044297°E)	5-Aug-15
	NK 270007	*Linognathoides urocitelli* n. sp.	Arkhangai	Zurkh Mountain (48.13280798°N, 100.098286°E)	21-Jul-15
	NK 272176	*Linognathoides urocitelli* n. sp.	Khovsgol	Heegtsar River Valley (48.90313899°N, 90.11070801°E)	19-Aug-15

Table 1. Mongolian host-sucking louse identifications with collection dates and localities.

Figure 1

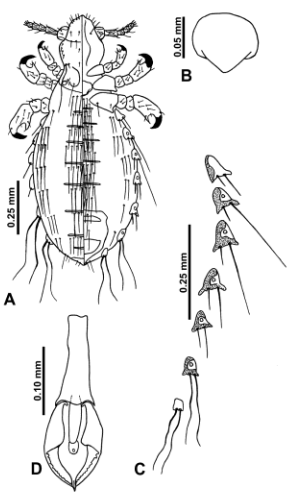

Figure 3

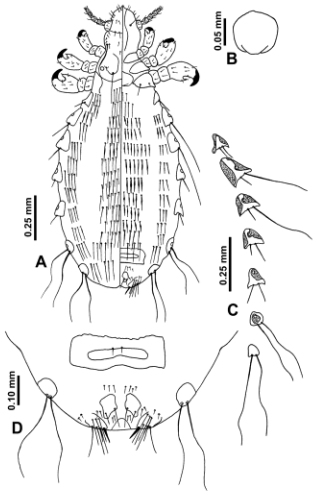

Figure 2

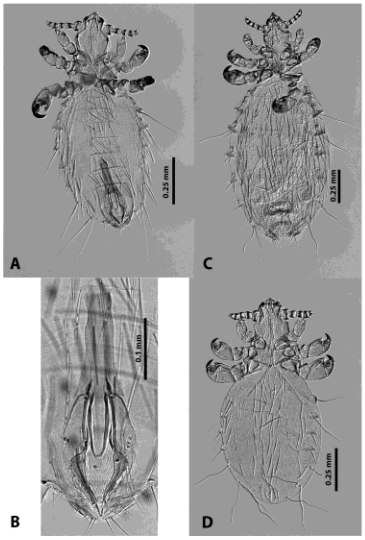

Figure 1. *Linognathoides urocitelli* n. sp., male. **(A)** Dorsoventral drawing of whole louse (dorsal features on left side, ventral features on right). **(B)** Thoracic sternal plate. **(C)** Paratergal plates. **(D)** Genitalia.

Figure 2. *Linognathoides urocitelli* n. sp. Differential interference contrast photomicrographs of cleared specimens. **(A)** Male. **(B)** Male genitalia. **(C)** Female (note sclerotized outline of egg inside abdomen). **(D)** Third instar nymph.

Figure 3. *Linognathoides urocitelli* n. sp., female. **(A)** Dorsoventral drawing of whole louse (dorsal features on left side, ventral features on right). **(B)** Thoracic sternal plate. **(C)** Paratergal plates. **(D)** Genitalia.

Description of Hoplopleura n. sp.

(Figs. 4)

Male (Fig. 4A, 4B) (n=9): Total body length of Holotype, 0.945 mm (mean, 0.916 mm; range, 0.878-1.028 mm). Head, thorax and abdomen moderately sclerotized.

Head: Longer than wide with broadly curved lateral margins posterior to antennae and extended medio-anteriorly; distinct dorsal lobe on each side posterior to head suture; maximum head width of Holotype, 0.150 mm (mean, 0.151 mm, range, 0.150–0.152 mm). Antennae 5-segmented with fairly broad basal segment and slightly elongated second segment; no antennal segments highly modified. 1 distinct VPHS, 2 Ventral Preantennal Seate (VPaHS), 2 Sutural Head Setae (SHS), 4 Dorsal Marginal Head Setae (DMHS), 2 Dorsal Anterior Head Setae (DAnHS), 1 Dorsal Anterior Central Head Seta (DAnCHS), 1 Dorsal Posterior Central Head Setae (DPoCHS), 1 Dorsal Principal Head Seta (DPHS), 1 small Dorsal Accessory Head Seta (DAcHS), 2 Supraantennal Head Setae (SpAtHS), 1 small Dorsal Preantennal Head Seta DPaHS), and 4-6 Apical Head Setae (ApHS) on each side.

Thorax: Broader than head; maximum thorax width of Holotype, 0.205 mm (mean, 0.211 mm; range, 0.205–0.216 mm). Thoracic sternal plate (Fig. 4B) somewhat shield shaped, with long posterior extension having squarish posterior margin, small anterior projection, and with small lateral indentation on each side. Thoracic fragma distinct. Mesothoracic spiracle diameter of Holotype, 0.016 mm (mean, 0.016 mm; range, 0.015–0.017 mm). Dorsal Principal Thoracic Seta (DPTS) length of Holotype, 0.103 mm (mean, 0.104 mm; range, 0.100 – 0.108 mm). Legs each terminating in tibio-tarsal acuminate claw; claw on hindlegs broader than claws on fore and midlegs; forelegs

slightly smaller than midlegs; midlegs slightly smaller than hindlegs; leg coxae variously shaped (Fig. 4B).

Abdomen: Broader than thorax with 13 tergites and 10 sternites. Tergites 1 and 3 fairly broad; tergite 1 partially separated medially; tergites 2 and 4 very broad each with diverging acuminate posterior-lateral margins; tergites 4-13 wider than previous tergites; tergite 13 distinctly curved. Sternites 1 and 2 broader than other sternites; sternites 2 and 3 each articulating laterally with corresponding paratergal plate (as characteristic of genus); sternites 3-10 each fairly narrow. Tergite 1 lacking Tergal Abdominal Setae (TeAS); tergites 2 and 3 each with 1 long TeAS and 1 very long TeAS on each side; tergites 4-12 each with 7-12 fairly long TeAS; tergite 13 with 4 small setae on each side 1 Dorsal Marginal Abdominal Seta (DMAS) lateral to tergites 5-12 on each side. Sternites 1 and 2 each with 7 long Sternal Abdominal Setae (StAS); 2 lateral StAS on each side of sternite 2 slightly diverging with medial of each of these pairs of StAS much more robust than lateral StAS. Sternites 3-10 each with 7-8 long StAS. 1 Ventral Marginal Abdominal Seta (VMAS) on each side lateral to each of sternites 5-13.

Paratergal plates (Fig. 4A, 4B): Present on abdominal segments 1-8. Plate I small and lacking apical setae. Plates II-V subtriangular; plate VI subrectangular; plates VII and VIII subeliptical. Plates III-VII each with small spiracle. Plates II-VI each with 2 Paratergal Setae (PrS) of moderate length; plates VII and VIII each with 2 very long PrS; Prs setae on plates II and III slightly thickened.

Genitalia: Basal apodeme sub equal in length to parameres and with moderately sclerotized, postero-lateral extensions. Parameres fairly straight in anterior section and then broadly curved. Pseudopenis with acuminate lateral extensions and extending

posteriorly well beyond posterior apices of parameres. Sub genital plate (Fig. 2) surface distinctly speculate and extending anteriorly to paratergal plate VI, with slightly concave anterior margin, sinuous lateral margins, tapering posteriorly, and differentially sclerotized as represented by 2 distinct horizontal bands; small central lacuna present anteriorly with 3 very long setae inserted along posterior margin; 2 very long setae inserted along posterior margin of middle sclerotized band.

Female (Fig. 4C, 4D). (n=7). Total body length of Allotype, 1.275 mm (mean, 1.264 mm; range, 1.198 – 1.345 mm).

Head, thorax and abdomen as in male unless indicated otherwise.

Head (Figs. 4C, 4D): Maximum head width of Allotype, 0.161 mm (mean, 0.161 mm; range, 0.161 – 0.162 mm).

Thorax (Figs. 4C, 4D): Maximum thorax width of Allotype, 0.230 mm (mean, 0.227 mm; range, 0.225 – 0.230 mm). Mesothoracic spiracle diameter of Allotype, 0.017 mm (mean, 0.017; range, 0.016 – 0.019). DPTS length of Allotype, 0.104 mm (mean, 0.105 mm; range, 0.102 – 0.108 mm). Thoracic sternal plate (Fig. 4D) with more rounded margin on posterior extension than male.

Abdomen: Broader than thorax with 19 tergites and 15 sternites. Tergites 1-4 as in male; tergites 5-18 narrow, each with 5-8 long TeAS; last distinctly tergite curved and with 1 short and 2 long setae on each side. Sternites 1 and 2 as in male; sternites 2 and 3 each articulating laterally with corresponding paratergal plate (as characteristic of genus); sternites 3-15 each fairly narrow and with 8-12 StAS. 1 DMAS on each side lateral to each of tegites 6-18. 1 VMAS on each side lateral to each of sternites 6-15.

Paratergal Plates (Fig. 4C, 4D): As in male but exact shape of some individual plates slightly different.

Genitalia (Fig. 4C, 4D): Subgenital plate subtriangular but with small indentation on each side that is more obvious in cleared, slide- specimens and posterior extension that tapers to truncate margin; patches of spicules evident especially near anterior and medial lateral margins; 3 rows of small to minute setae in central to posterior region of plate, row 1 with 4-5 setae, rows 2 and 3 each with 2 setae. Gonopods VIII slightly elongate and medially situated, each with 3 posterior setae, antero-medial seta slightly shorter than other setae. Gonopods IX less distinct and slightly more lateral than gonopods VIII, each with 3 robust apical setae.

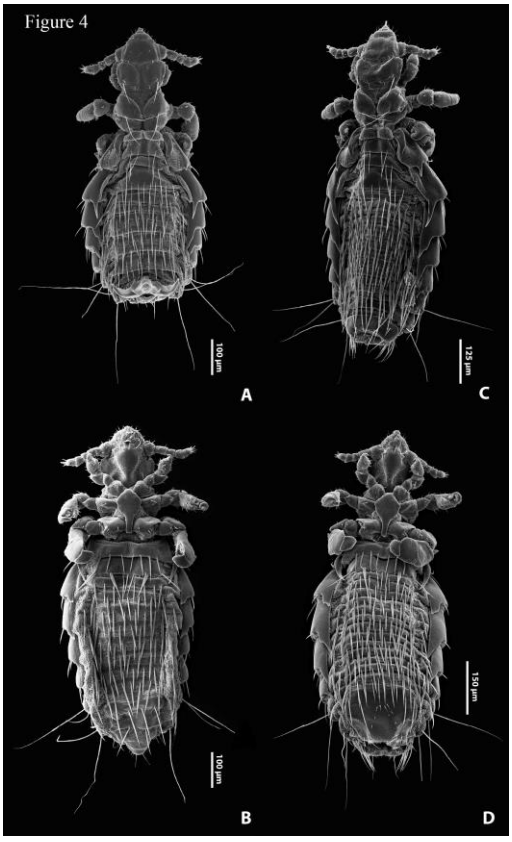

Figure 4. *Hoploplerua* n. sp. Scanning Electon Microscopy images of specimens. **(A)** Male dorsal. **(B)** Male ventral. **(C)** Female dorsal. **(D)** Female ventral.

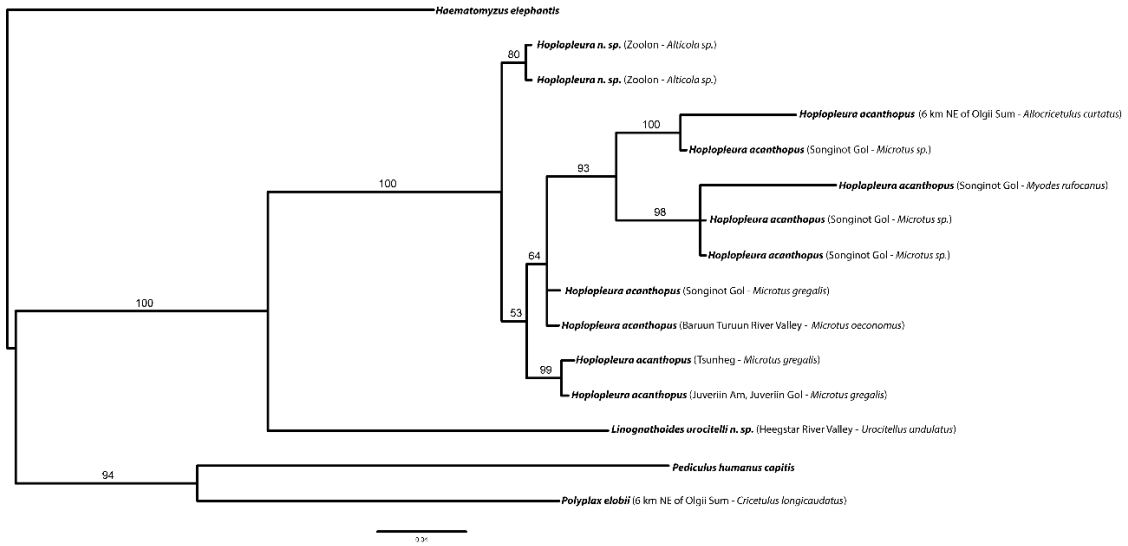

Figure 5. Phylogenetic relationships of 13 Mongolian sucking lice resulting from Bayesian analysis of concatenated gene fragments 16S rrnL and 12S rrnS.

Discussion

We have identified a new species of sucking louse belonging to the genus *Hoplopleura* from *Alticola barakshin* and *Alticola strelzowi*. Scanning electron microscopy was used for imaging both male and female specimens of this new species, alongside the slide mounted exoskeletons in the species description and measurements. We have also identified a new species of sucking louse within the genus *Linognathoides* from *Urocitellus undulatus*. The long-tailed ground squirrel is a Palearctic sciurid that ranges from eastern Kazakhstan to southern Siberia, northern and central Mongolia, and Heilungjiang province and Xinjiang autonomous region in northern China (Thorington and Hoffmann, 2005). Species descriptions included the use of Digital Light Microscopy Imaging and traditional light microscopy. For both new species, there will be submission of the Holotype male, Allotype female, and paratypes to the Museum of Southwestern Biology at the University of New Mexico in Albuquerque. The remaining lice were identified using light microscopy as well as genetic comparison using the Basic Local

Alignment Search Tool (BLAST) from the National Center for Biotechnology Information (NCBI). Along with identification, determination of lice with newly recorded hosts was completed by comparison to known references.

The discovery of these new species sheds new light on the host-parasite relationships of this area of the world. The large host range of *Hoplopleura* n. sp., residing prominently in North-Western Mongolia, can indicate that there can be multiple other unidentified new species from these hosts. According to the International Union for Conservation of Nature (IUCN 2019) red list, the hosts have various geographical ranges including Central Kazakhstan (*Alticola strelzowi*) and Southern Mongolia (*Alticola barakshin*). Future collections from these regions from these hosts will allow for a more thorough understanding of louse distribution and other parasitized hosts. *Linognathoides urocitelli* n. sp. could potentially range as far north as Central Russia, based on the distribution of its host as defined by the IUCN red list. No other known localities besides Western Mongolia are currently known for these new species of lice. A new species of *Polyplax* was identified; however, a formal description was not prepared because no male specimens were available for study.

The use of a SEM allowed for the enlightenment of an interesting dilemma. Traditionally, new species of sucking lice have been described using light microscopy. Due to the use of clearing agents, only well sclerotized areas of the exoskeleton are easily visible with the light microscopy. By comparison with SEM images, specifically the female subgenital plate of the *Hoplopleura* n. sp., a difference in shape can be seen between the imaging types. The SEM visualized a sub genital plate more curved laterally, whereas the light microscopy showed the sub genital plate having a lateral divergence.

When analyzing the female subgenital plate with the SEM, the areas identified by the light microscopy can be seen; however, where the light microscopy shows a lateral divergence, the SEM visualizes that area as a trough between two areas of higher sclerotization. Areas, such as the one previously discussed, can potentially be incorrect for new species of sucking lice that were only described using light microscopy. This indicates that SEM images allow for morphologically correct new species descriptions to be made.

Due to a lack of substantial molecular data, most of the DNA sequences from these taxa were obtained for the first time. The 16S and 12S DNA fragments obtained from the louse specimens, are the first for lice of this region of the world. When searching for viable gene sequences for phylogenetic inclusion, sequences were either non-existent or showed large gap regions deeming them unusable. This last aspect was of high relevance for the 18S DNA fragments. Unfortunately, the region of the 18S rRNA that was sequenced from extracted DNA showed to be a highly variable region with large areas of insertions and deletions. Due to this aspect, a phylogeny was not able to be created for these DNA fragments.

The molecular phylogenetic analysis includes for the first time individuals of *Hoplopleura* n. sp., *Linognathoides urocitelli* n. sp, *Polyplax elobii*, and *Hoplopleura acanthopus*. Specimens of *Hoplopleura* n. sp. show to be most closely related to its sister clade of collected specimens from the genus *Hoplopleura*. This reinforces our new species as being a member of the *Hoplopleura* genus, but different genetically from *Hoplopleura acanthopus*, forming a sister clade to the new species. Morphological differences seen in the new species description can be linked to the noticed genetic

differences. In continuation, the large *Hoplopleura* clade shows genetic relatedness to geographic location rather than specific host. Lice identified from the host genus *Microtus* appear to have genetic variability, reinforcing that individuals collected from the same or near geographic localities are more closely related. *Hoplopleura acanthopus* collected from Songinot Gol are more closely related to other *Hoplopleura acanthopus* collected from that locality rather than host. *Linognathoides urocitelli* n. sp. is most sister to *Hoplopleura*.

This molecular phylogeny coincides with that of Light, et. al (2010). *Polyplax* forms a sister clade with *Pediculus* and *Linognathoides* forms a sister group with *Hoplopleura*. Individuals of *Hoplopleura acanthopus, Polyplax elobii* and both new species were not included in the comparative phylogeny, therefore this phylogeny allows for an evolutionary linkage to be created from known Anoplura and our specimens of Mongolia.

In continuation, due to the genetic template of about 240 base pairs and non-reliable GenBank references, this phylogeny is limited. The concatenated phylogeny of 16S and 12S still allowed for proper Bayesian analysis, however future genetic work will be required to enhance this molecular database and create more in depth phylogenies.

Literature Cited

Barker, S. C., M. Whiting, K. P. Johnson, and A. Murrell. 2003. Phylogeny of the lice (Insecta, Phthiraptera) inferred from small subunit rRNA. Zoologica Scripta **32**: 407-414.

Cook, J. A., K. Galbreath, K. C. Bell, M. L. Campbell, S. Carriere, J. P. Colella, N. G. Dawson, J. L. Dunnum, R. P. Eckerlin, S. E. Greiman, et al. 2017. The Beringian

Coevolution Project: holistic collections of mammals and associated parasites reveal novel perspectives on evolutionary and environmental change in the north. Arctic Science 3: 585-617.

Dong, W., Song, S., Jin, D., Guo, X. and Shao, R. 2014. Fragmented Mitochondrial Genomes of the Rat Lice, *Polyplax asiatica* and *Polyplax spinulosa*: Intra-Genus Variation in Fragmentation Pattern and a Possible Link Between the Extent of Fragmentation and the Length of Life Cycle. BMC Genomics 15: 44

Durden, L. A., S. E. Kessler, U. Radespiel, E. Zimmermann, A. F. Hasiniaina, and S. Zohdy 2018. A new species of sucking louse (Phthiraptera: Anoplura: Poyplacidae) from the gray mouse lemur, *Microcebus murinus* (Primates: Cheirogaleidae), in Madagascar. Journal of Medical Entomology 55: 910-914.

Durden, L., Musser, G. 1994. The Mammalian Hosts of the Sucking Lice (Anoplura) of the World: A Host-Parasite List. Bull. Soc. Vector Ecol. 19(2): 130-168.

Galbreath, K. E., E. P. Hoberg, J. A. Cook, K. C. Bell, M. L. Campbell, J. L. Dunnum, R. P. Eckerlin, S. L. Gardner, S. E. Greiman, H. Henttonen, et al. 2019. Field collection of parasites from mammals: building an integrated infrastructure for investigating biodiversity. 100: Gerwel, C. 1954. Materialy do fauny wyzy (Anoplura) Polski. Acta Parasitologica Polonica 2: 171-208.

IUCN 2019. *The IUCN Red List of Threatened Species. Version 2019-1*. http://www.iucnredlist.org.

Kéler, S. 1967. Über Einige Mallophagen Und Läuse Aus Der Mongolei. Ergebnisse der Mongolisch-Deutschen Biologischen Expedition seit 1962, Nr. 29. Mitt. Zool. Mus. Berlin 43: 247-250.

Kim, K. C., and H. W. Ludwig. 1978. The family classification of the Anoplura. Systematic Entomology 3: 249-284.

KRIŠTOFŠÍK, J. 1999. Sucking Lice (Phthiraptera) from Mongolian Mammals. Biologia, Bratislava 54/2: 143-149.

Light, J., Smith, V., Allen, J., Durden, L., Reed, D. 2010. Evolutionary history of mammalian sucking lice (Phthiraptera: Anoplura). BMC Evolutionary Biology 10:292

Sikes, R. S., W. L. Gannon, and the Animal Care and Use Committee of the American Society of Mammalogists. 2011. Guidelines of the American Society of Mammalogists for the use of wild mammals in research. Journal of Mammalogy 92: 235-253.

Thorington, Jr., R. W., and R. S. Hoffmann. 2005. Family Sciuridae. *In* Mammal Species of the World: A Taxonomic and Geographic Reference, 3rd edition., D. E. Wilson and D. M. Reeder (eds.). The Johns Hopkins University Press, Baltimore, Maryland. p. 754-818.

Tkach, V.V., and J. Pawlowski, A new method of DNA extraction from the ethanol-fixed parasitic 461 worms, Acta Parasitol. 44 (1999) 147–148.